

Oxygen Permeation through Thin Mixed-Conducting Solid Oxide Membranes

Yue-Sheng Lin, Weijian Wang, and Jonghee Han

Dept. of Chemical Engineering, University of Cincinnati, Cincinnati, OH 45221

A new approach for developing fundamental equations of oxygen permeation through thin mixed-conducting oxide ceramic is presented considering both surface reactions on membrane-gas interfaces and the diffusion of charged species in the bulk oxide. The essence of this work is the coupling of surface reactions with the bulk diffusion using a novel approach which differs from the conventional Wagner theory applicable only to limited cases. With this approach, fundamental equations based on various permeation mechanisms can be derived for oxygen permeation through thin mixed-conducting oxide membranes, which is impossible using conventional approach. In general, the final results are a complex implicit equation correlating the oxygen permeation flux to the driving force, membrane thickness, and rate constants with physical significance in each step. Somewhat simpler theoretical oxygen permeation equations are obtained for some special cases (mixed-conducting membranes with a rate-limiting step, ionic-conducting membranes, ionic-conducting membranes with a reducing agent in permeate side). Theoretical results derived using this new approach agree excellently with the experimental oxygen permeation data. It is theoretically and experimentally shown that for ionic conductors, the surface permeation parameter measured by the dynamic permeation method is directly related to the oxygen isotope exchange rate constant measured under equilibrium conditions.

Introduction

Inorganic membranes have recently attracted considerable interest in the scientific community (Burggraaf et al., 1989; Bhawe, 1991). An emerging group of ceramic membranes are those made of dense fast ionic ceramic conductors which have a very large permselectivity for oxygen (Burggraaf et al., 1991; Lin, 1992). Conventionally, these materials are used as electrolytes (ionic conductors) and, in some cases, as electrodes (mixed conductors) for solid oxide fuel cells and oxygen sensors (Steele, 1987). The use of these fast ionic conductors as oxygen semipermeable membranes is stimulated mainly by the structural simplicity of such a membrane device, for which no electrodes and external electric connectors are required as compared to the fuel cells.

Oxygen permeation (normally at elevated temperature) through a dense solid oxide membrane is defined as a flux of neutral oxygen passing through a unit permeating area of the

film imposed with an oxygen chemical potential gradient. Studies on the oxygen permeation through the membranes made of these fast-ionic conductors, especially when they are very thin, are essential to the fabrication and practical application of these dense ceramic membranes. Understanding of the permeation mechanisms involved in the oxygen transport through these dense ceramic membranes is also important to oxygen sensors, oxygen pumps, solid oxide fuel cells, and membrane reactors for partial oxidative reactions. For example, the electrochemical vapor deposition process, a technique used to fabricate thin electrolyte layers for solid oxide fuel cells (Isenburg, 1982; Carolan and Michaels, 1990; Pal and Singhal, 1990; Lin et al., 1990) relies essentially on the oxygen permeation through the fast ionic conducting electrolyte materials.

Oxygen permeation through a fast ionic-conductor is a result of oxygen ionic conduction using mechanisms that involve defects such as lattice vacancies and interstitial atoms. Under the influence of thermal agitation, these defects move ran-

Correspondence concerning this article should be addressed to Y.-S. Lin.

domly within the lattice. If certain unbalanced force (electric field or pressure gradient) acts on the mobile species, this random motion can be biased to produce a net drift motion. Therefore, if a fast ionic conductor is imposed by the electric field or by the pressure gradient of the gas of mobile species in the conductor, the ions can move in one direction, resulting in a net ionic flux through the conductor. In the absence of macroscopic electric field, the ionic lattice should be neutral everywhere. This overall charge neutrality requires that one type of charged defect (for example, oxygen vacancies) must be compensated by a second type of defect of opposite sign (for example, electrons). Ceramic materials exhibiting both the ionic and electronic conductivities are referred to as the mixed conductors (Heyne, 1977; Kofstad, 1972).

The oxygen ion conduction in relatively thick layers of the fast ionic conductors has been extensively studied because it is directly related to metal corrosion and many other applications where these materials are used as electrolyte or electrodes (Heyne, 1968, 1977; Kofstad, 1966, 1972). In comparison, studies on oxygen permeation through thin dense ceramic membranes made of the fast ionic conductors are very limited. This is in part because using the mixed-conducting materials as thin ceramic membranes is a relatively new concept, and until recently most theoretical work in these areas has been focused on the oxygen transport in electrolytes and electrodes. The difficulty of fabricating gas-tight thin mixed-conducting oxide membranes of different thickness and the problems (for example, high-temperature sealing) associated with high temperature oxygen permeation experiments might be also responsible for the limited studies on oxygen permeation through dense ceramic membranes.

It has been recently recognized that the oxygen permeation through a mixed-conducting membrane consists of several steps (Dou et al., 1985; Bouwmeester, 1991; Lin et al., 1990). In Figure 1 an oxide membrane is schematically divided into the bulk oxide and the adjacent interfaces, emphasizing both solid state diffusion and surface electrochemical reactions in the mass transport of the oxygen species. Among the limited experimental studies on oxygen permeation through fast ionic conductors, almost all studies focused on the oxygen permeation through relatively thick ($> 500 \mu\text{m}$) stabilized zirconia films which are essentially ionic conductors (Alcock and Chan, 1972; Palguez et al., 1972; Fouletier et al., 1976; Dou et al., 1985; Park and Blumenthal, 1989; Bouwmeester et al., 1992). In these studies, most researchers considered only the oxygen transport through the bulk oxide. The oxygen permeation flux could be described by the equation derived from the Wagner theory, which assumes the oxygen transport in the bulk oxide being the rate limiting step (Heyne, 1968, 1977; Kofstad, 1966, 1972).

The basic assumption made in the Wagner theory is the existence of a local equilibrium between the two charged species (for example, oxygen ion and electron) and a hypothetical neutral species (for example, molecular oxygen) in the bulk oxide (Heyne, 1977) (see Appendix). The resulting oxygen permeation flux (in mole of molecular oxygen) can be described by (Heyne, 1977; Gellings and Bouwmeester, 1992):

$$J_{O_2} = \frac{1}{4F^2L} \int_{\mu_{O_2}^{(II)}}^{\mu_{O_2}^{(I)}} t_i t_n \sigma_i d\mu_{O_2} \quad (1)$$

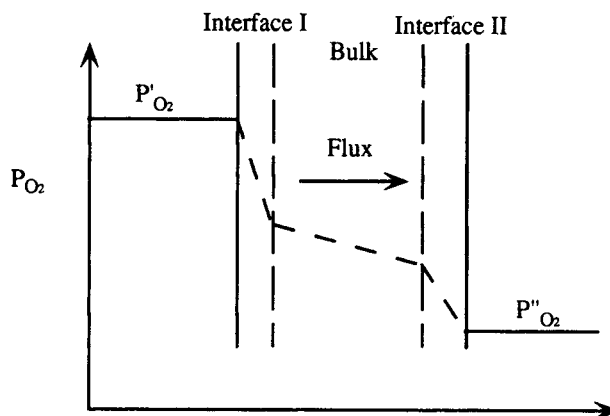


Figure 1. Oxygen transport through an oxide membrane.

where t_i and t_n are respectively the oxygen ionic and electronic transfer numbers; σ_i is the total conductivity and μ_{O_2} is the chemical potential of the hypothetical neutral oxygen in the oxide. For ionic conductors ($t_i \approx 1$) and assuming an ideal thermodynamic behavior for the species involved, Eq. 1 is reduced to:

$$J_{O_2} = \frac{RT}{4F^2L} \int_{P''_{O_2}}^{P'_{O_2}} \sigma_n d(\ln P_{O_2}^*) \quad (2)$$

where σ_n is the electron conductivity which is a function of oxygen partial pressure and $P_{O_2}^*$ is the partial pressure of the hypothetical neutral molecular oxygen in the bulk oxide. In the Wagner theory, this hypothetical pressure on the surface of the oxide becomes the same as the oxygen partial pressure in the ambient atmosphere. When electron-hole conduction is primarily responsible for the electronic conductivity, which, as a result, is proportional to $P_{O_2}^{1/4}$, the oxygen permeation flux can be correlated to the oxide thickness L and oxygen pressures in the two ambient atmospheres by (Dou et al., 1985; Park and Blumenthal, 1989):

$$J_{O_2} = \frac{\beta}{L} (P_{O_2}'^{1/4} - P_{O_2}''^{1/4}) \quad (3a)$$

with

$$\beta = \frac{RT\sigma_p^0}{4F^2} \quad (3b)$$

where σ_p^0 is the electron-hole conductivity of the materials exposed to an atmosphere of 1 atm oxygen partial pressure.

Equation 3 has been used to describe the experimentally measured oxygen permeation fluxes. Indeed for the thick oxide films the experimental results are consistent with the theoretical prediction (Alcock and Chan, 1972; Palguez et al., 1972; Fouletier et al., 1976; Dou et al., 1985; Park and Blumenthal, 1989; Bouwmeester et al., 1992). It is obvious, however, that the surface charge transfer reactions can be very important when the oxygen transport resistance in the bulk oxide becomes very small as a result of the increase in ionic and electronic conductivities or the decrease in film thickness. Applications

of the fast ionic conductors as ceramic membranes are closely related to these cases, in which both the surface reactions and bulk diffusion should be considered.

Dou et al. (1985) appear to be the first to consider both the surface reaction step and the bulk diffusion step in oxygen permeation through calcia-stabilized zirconia films (an ionic conducting oxide). Neglecting the surface reaction resistance in interface II (lower oxygen pressure side), they proposed the following two equations to describe the oxygen permeation flux:

$$J_{O_2} = \alpha (P_{O_2}^{'1/2} - P_{O_2(l)}^{1/2}) \quad (4)$$

$$J_{O_2} = \frac{\beta}{L} (P_{O_2(l)}^{1/4} - P_{O_2}''^{1/4}) \quad (5)$$

where α is the surface permeation constant and $P_{O_2(l)}$ is the oxygen partial pressure of the hypothetical molecular oxygen in the oxide at the interface I. Equation 4 accounts for the surface reaction and Eq. 5 is derived from Eq. 3 based on the Wagner theory. Considering both surface reactions steps, Bouwmeester et al. (1992) recently used the following three correlations to describe the oxygen permeation through oxide membranes:

$$J_{O_2} = \alpha (P_{O_2}^{'5/8} - P_{O_2(l)}^{5/8}) \quad (6)$$

$$J_{O_2} = \frac{\beta}{L} (P_{O_2(l)}^{1/4} - P_{O_2(l)}^{1/4}) \quad (7)$$

$$J_{O_2} = \alpha (P_{O_2(l)}^{5/8} - P_{O_2}''^{5/8}) \quad (8)$$

Equations 4 and 5 and Eqs. 6–8 could describe well the experimental data reported by Dou et al. (1985) and Bouwmeester et al. (1992). Nevertheless, these equations (especially the ones for the surface reactions) were employed as empirical equations, as also pointed out by Bouwmeester et al. (1992). As a result of the empirical nature, the physical meaning of the parameter α and the order (1/2 or 5/8) on the oxygen partial pressure in these equations is not certain. The lack of the theoretical equations with physical significance for oxygen permeation through thin dense oxide membranes is mainly due to the unavailability of a theoretical approach which allows coupling the surface reaction with the bulk diffusion. The well-established Wagner theory has been proven to work well for oxygen permeation through thick dense oxide membranes in which the bulk diffusion is the rate-limiting step. However, it is difficult, if not impossible, to use the conventional Wagner approach to establish the rate equations for the surface reactions and to integrate the surface reaction equations with the bulk diffusion equations.

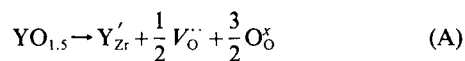
Recently, there has been a growing interest in fabrication and application of thin fast ionic-conducting ceramic membranes for various novel processes. These processes include oxygen separation using thin oxygen semipermeable ceramic membranes (Burggraaf et al., 1991; Burggraaf and Lin, 1992; Gür et al., 1992), electrochemical vapor deposition of solid electrolyte films for fuel cells and oxygen sensors (Isenburt, 1981; Brian, 1989; Carolan and Michaels, 1990; Lin et al., 1990), and oxidative chemical reactions using dense oxide

membrane reactors (Hazbun, 1988; 1989; Hsieh, 1991; Gelling and Bouwmeester, 1992). Both the surface reactions and the bulk diffusion are important in the oxygen permeation through the membranes used in these processes. Obviously, urgent needs exist for the development of a theoretical approach on which fundamental equations can be derived to correlate the oxygen permeation flux through thin fast ionic-conducting ceramic membranes. The objectives of this article are: (1) to report a new approach which allows establishing the rate equations for the surface reactions and bulk diffusion in mixed-conducting solid oxide membranes and integrating the surface reaction equations with the bulk diffusion equations; and (2) to demonstrate the applications of this new approach for derivation of fundamental equations correlating the oxygen permeation flux to the driving force and rate constants with physical significance.

Theoretical Development

As shown in Figure 1, the oxygen permeation through a mixed-conducting solid oxide membrane involves the following rate steps: (1) reduction surface reaction on interface I; (2) diffusion of charged species in the bulk oxide; and (3) oxidation surface reaction on interface II. The surface reactions may involve several sub-steps, such as adsorption or desorption of oxygen and charge transfer reactions. In what follows, the bulk diffusion and surface reaction equations are derived using the new approach which is very different from the conventional Wagner method. With this approach, the bulk diffusion equation can be readily coupled with the surface reaction rate equations for mixed-conducting solid oxide membranes. The final results of these theoretical analysis are implicit (or explicit in some cases) equations which correlate the oxygen permeation flux to the oxygen partial pressures in the both sides of membranes, the membrane dimension and the rate constants with physical significance.

To demonstrate this approach, we focus on the transport of two charged species in the bulk oxide. One typical charged species is the oxygen vacancy, $V_O^{\bullet\bullet}$, which can be created by, for example, doping a lower valence oxide (for example, Y_2O_3) into a higher valence oxide (for example, ZrO_2) as:



The Kröger-Vink notation (Kröger and Vink, 1956) is used in reaction A and for other electrochemical reaction processes described in this article. In the bulk oxide, the oxygen vacancy moves from the lower P_{O_2} side to the higher P_{O_2} side, expressed as:



The other charge balancing species can be either electron-hole or electron, whichever present depends on the membrane materials and oxygen pressure range. The electron transport directions are indicated by:



or

$$e'_{(II)} \rightarrow e'_{(I)} \quad (D)$$

Under steady state, the flux of charged species 1 (for example, the oxygen vacancy) can be described by:

$$J_1 = -D_a \nabla C_1 \quad (9)$$

$$D_a = \frac{(z_1^2 f_1 C_2 + z_2^2 f_2 C_1) D_1 D_2}{z_1^2 C_1 D_1 + z_2^2 C_2 D_2} \quad (10)$$

$$f_i = \frac{\partial \ln a_i}{\partial \ln C_i} \quad (i = 1 \text{ or } 2) \quad (11)$$

The derivation of Eqs. 9 and 10 is given in the Appendix. f_i in Eq. 11 is called the thermodynamic factor (Heyne, 1977). In general, f_i is a function of the concentrations of the mobile charged species (C_1 , C_2). Equation 9 has the form of Fick's law, but the apparent diffusivity D_a is a complex function of the concentrations of the two mobile charged species (note that the thermodynamic factor f_1 and f_2 are also functions of C_1 and C_2). Oxygen permeation through membrane is normally one-dimensional, so Eq. 9 can be written as:

$$J_1 = -D_a \frac{dC_1}{dl} \quad (12)$$

or

$$J_1 = -\frac{1}{L} \int_{C_{(I)}}^{C_{(II)}} D_a dC_1 \quad (13)$$

where subscripts (I) and (II) indicate the concentrations of the mobile charged species on interfaces I and II (still in the oxide), respectively.

The local electroneutrality requirement gives (see Appendix):

$$z_1 C_1 + z_2 C_2 = z_1 C_1^0 + z_2 C_2^0 \quad (14)$$

where C_i^0 ($i = 1$ or 2) is the equilibrium concentration of mobile charged species i when the oxide membrane is equilibrated to an ambient atmosphere of $P_{O_2} = 1$ atm. It should be mentioned that when the solid oxide membrane gets very thin, the local electroneutrality assumption may be no longer valid. However, it is not known at what membrane thickness the assumption breaks down. This critical thickness depends on the membrane materials and oxygen permeation conditions. To understand that requires extensive experimental study. Nevertheless, using the assumption of local electroneutrality is the starting point of developing theories for oxygen permeation through thin dense oxide membranes.

If the concentration dependence of f_1 and f_2 is known, the integration in Eq. 9 becomes possible with the use of Eq. 14 to eliminate C_2 in D_a . Thus, the flux J_1 is finally correlated to D_1 , D_2 , C_1^0 , and C_2^0 , which are the properties of membrane, and $C_{1(I)}$, $C_{1(II)}$, $C_{2(I)}$, and $C_{2(II)}$, which can be coupled to the equations describing the surface reactions. Analytical expression correlating J to $C_{1(I)}$, $C_{1(II)}$, $C_{2(I)}$, and $C_{2(II)}$ depends on the function of $f_i(C_1, C_2)$ and is difficult to obtain for the general cases. To simplify the presentation of this new approach, we only consider mixed-conducting oxide with an ideal behavior

($f_i = 1$). It should be pointed out that the approach reported here is applicable to the mixed-conducting oxide with a non-ideal behavior.

For mixed-conducting membranes with the oxygen vacancy and electron hole as the mobile charged species, the oxygen permeation process can be described by reactions B and C. Considering the oxygen vacancy as species 1 and the electron-hole as species 2, we can write Eq. 13 with Eq. 10 in the following form with subscripts V and p replacing subscripts 1 and 2 (note $z_1 = 2$ and $z_2 = 1$):

$$J_V = -\frac{1}{L} \int_{C_{V(I)}}^{C_{V(II)}} \frac{(C_p + 4C_V) D_V D_p}{4C_V D_V + C_p D_p} dC_V \quad (15)$$

Note $f_i = 1$ for species with an ideal behavior. With the same notation, Eq. 14 can be written as:

$$2C_V + C_p = 2C_V^0 + C_p^0 \quad (16)$$

Inserting Eq. 16 into Eq. 15 to eliminate C_p and then integrating Eq. 15 with respect to C_V gives:

$$J_{O_2} = \frac{D_V D_p}{2L} \left(\frac{C_{V(II)} - C_{V(I)}}{2D_V - D_p} + \frac{C_p^0 (D_V - D_p)}{(2D_V - D_p)^2} \ln \frac{4D_V C_{V(II)} + D_p C_{p(II)}}{4D_V C_{V(I)} + D_p C_{p(I)}} \right) \quad (17a)$$

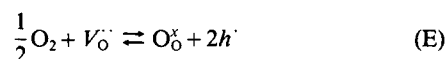
or, with the Einstein's relation, $\sigma_i = (z_i^2 F^2 / RT) C_i D_i$

$$J_{O_2} = \frac{RT}{8F^2 L (2r_p - 1)^2} \left[(2r_p - 1)(\sigma_{V(II)} - \sigma_{V(I)}) + (r_p - 1)(2\sigma_V^0 + 4\sigma_p^0 r_p) \ln \frac{\sigma_{V(II)} + \sigma_{p(II)}}{\sigma_{V(I)} + \sigma_{p(I)}} \right] \quad (17b)$$

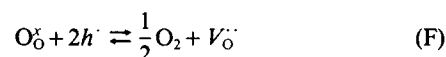
with $C_p^0 = 2C_V^0 + C_p^0$ and $r_p = D_V / D_p$. Note that in Eq. 17, J_{O_2} is the mole flux of molecular oxygen: $J_{O_2} = -1/2 J_V$. Equation 17 correlates the oxygen permeation flux to $C_{V(I)}$ and $C_{V(II)}$.

The surface reactions on the two interfaces of the mixed-conducting membranes can be written in the following general forms:

On interface I



On interface II



Physically, reaction E means that the molecular oxygen (in the higher pressure side) is incorporated into the oxygen vacancy and releases two electron holes on interface I, and reaction F means that the lattice oxygen, getting two electron holes, becomes the molecular oxygen (in the lower pressure side) by releasing one oxygen vacancy. In fact, the surface reactions may involve many substeps, such as oxygen molecular

adsorption, dissociation of adsorbed oxygen molecules, and charge transfer, resulting in the existence of several intermediates ($O_{2,ads}$, O_{ads} , and O_{ads}^-) (Robertson and Michaels, 1987; Boukamp et al., 1989b; van Hassel, 1990). If we neglect the substeps in the surface reactions, and consider reactions E and F as the elementary reactions, application of the mass action law (Kingery, 1976) gives:

On interface I

$$J_{O_2} = K_1 C_{V(I)} P_{O_2}'^{1/2} - K_{-1} C_{p(I)}^2 \quad (18)$$

On interface II

$$J_{O_2} = K_{-1} C_{p(II)}^2 - K_1 C_{V(II)} P_{O_2}''^{1/2} \quad (19)$$

where K_1 and K_{-1} are forward and backward reaction rate constants for the surface (charge transfer) reactions E and F. The lattice oxygen concentration is incorporated into rate constant K_{-1} as it is essentially a constant.

Equations 18 and 19 correlate the oxygen permeation flux to the surface reaction rate constant, and $C_{V(I)}$, $C_{V(II)}$, $C_{p(I)}$, $C_{p(II)}$, P_{O_2}' , and P_{O_2}'' . If we consider several substeps for the surface reactions and apply the mass action law to each substep, we can in principle obtain the final equations which correlate the oxygen permeation flux to the rate constants in each substep, and $C_{V(I)}$, $C_{V(II)}$, $C_{p(I)}$, $C_{p(II)}$, P_{O_2}' , and P_{O_2}'' (see Comparison with Experimental Data section). In such cases, the final results can be very complicated, but the basic principles shown here for the simpler case still apply. Equations 17–19 contain five variables (J_{O_2} , $C_{V(I)}$, $C_{V(II)}$, $C_{p(I)}$, $C_{p(II)}$). Application of Eq. 16 on the two interfaces will result in two additional equations:

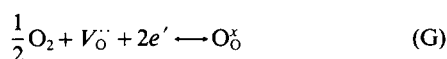
$$2C_{V(I)} + C_{p(I)} = 2C_V^0 + C_p^0 \quad (20)$$

$$2C_{V(II)} + C_{p(II)} = 2C_V^0 + C_p^0 \quad (21)$$

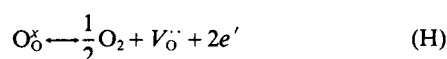
The solutions of Eqs. 17–21, by eliminating $C_{V(I)}$, $C_{V(II)}$, $C_{p(I)}$, and $C_{p(II)}$, give an implicit equation which correlates the oxygen permeation flux to P_{O_2}' , P_{O_2}'' , the rate constants, and the membrane thickness.

In the case that the electron, instead of electron hole, contributes primarily to the electric conduction of an oxide membrane, the surface reactions are:

On interface I:



On interface II:



For the bulk diffusion transport (reactions B and D), we can follow the same procedure as given above and derive the following equation for the oxygen permeation flux in the bulk oxide:

$$J_{O_2} = \frac{D_n D_V}{2L} \left[\frac{3(C_{V(II)} - C_{V(I)})}{D_n + 2D_V} + \frac{(2C_V - C_n)(D_n - D_V)}{(D_n + 2D_V)^2} \ln \frac{C_{n(II)} D_n + 4C_{V(II)} D_V}{C_{n(I)} D_n + 4C_{V(I)} D_V} \right] \quad (22a)$$

or

$$J_{O_2} = \frac{RT}{8F^2 L (2r_n + 1)^2} \left[3(2r_n + 1)(\sigma_{V(II)} - \sigma_{V(I)}) + (2\sigma_V^0 - 4r_n \sigma_n^0)(1 - r_n) \ln \frac{\sigma_{n(II)} + \sigma_{V(II)}}{\sigma_{n(I)} + \sigma_{V(I)}} \right] \quad (22b)$$

with $r_n = D_V/D_n$. Note that in this case, subscript n has replaced subscript 2 and $z_2 = -1$. Assuming that reactions G and H are primary reactions, application of the mass action law for these two surface reactions gives:

$$J_{O_2} = K_n C_{V(I)} C_{n(I)}^2 P_{O_2}''^{1/2} - K_{-n} \quad (23)$$

and

$$J_{O_2} = K_{-n} - K_n C_{V(II)} C_{n(II)}^2 P_{O_2}'^{1/2} \quad (24)$$

Again, solutions of Eqs. 21–24 together with the two equations derived from Eq. 14 on interface I and II give another implicit equation correlating the oxygen permeation flux to P_{O_2}' , P_{O_2}'' , the rate constants, and the membrane thickness.

The fundamental equations presented in this section show that the oxygen permeation through a mixed-conducting solid oxide depends on the driving force (oxygen partial pressures in both sides), the electrochemical transport mechanism (electron or electron-hole conduction), the initial defect concentrations, the rate constants associated with each rate step, and the oxide film thickness. It is difficult to find the explicit expression correlating the permeation flux to those parameters, as just mentioned. Thus for mixed-conducting dense membranes, the dependence of the permeation flux on the oxygen partial pressure and temperature is rather complex, depending on the specific surface reaction steps and the values of the rate parameters involved.

Oxygen Permeation Equations for Special Cases Mixed-conducting membranes with a rate-limiting step

For the membranes with a thickness or small ionic and electron-hole conductivities, the diffusion in the bulk oxide becomes the rate-limiting step. In this case, assuming quasi-equilibrium in the two surface reaction steps, Eq. 18 and Eq. 19 become:

$$K_1 C_{V(I)} P_{O_2}'^{1/2} = K_{-1} C_{p(I)}^2 \quad (25)$$

$$K_1 C_{V(II)} P_{O_2}''^{1/2} = K_{-1} C_{p(II)}^2 \quad (26)$$

Solution of Eq. 25 and Eq. 26, together with Eq. 20 and Eq. 21 gives four complex expressions correlating $C_{V(I)}$, $C_{V(II)}$, $C_{p(I)}$, and $C_{p(II)}$ to P_{O_2}' , P_{O_2}'' , C_V^0 , C_p^0 , K_1 , and K_{-1} , respectively, which

can be inserted into Eq. 17. The final result is an explicit, but fairly complex equation.

The following equations similar to Eq. 25 and Eq. 26 can be found from Eq. 23 and Eq. 24 for the membranes in which the electron, not electron hole, contributes primarily to the electronic conductivity:

$$K_1 C_{V(l)} C_{n(l)}^2 P_{O_2}^{\prime 1/2} = K_{-1} \quad (27)$$

$$K_1 C_{V(l)} C_{n(l)}^2 P_{O_2}^{\prime \prime 1/2} = K_{-1} \quad (28)$$

An implicit equation can be derived which correlates the permeation flux to P_{O_2}' and P_{O_2}'' and other parameters. In general, for mixed-conducting membranes the dependence of the permeation flux on the oxygen partial pressure is complicated even in the simpler cases that the diffusion in the bulk oxide is the rate-limiting step.

For the very thin membrane with electron holes contributing mainly to electronic conduction, the surface reactions may become rate-limiting. In this case, $C_{p(l)} \approx C_{p(l)}$, $C_{V(l)} \approx C_{V(l)}$. The solution of Eq. 18, Eq. 19 with Eq. 20 (or Eq. 21) gives:

$$J_{O_2} = \alpha (P_{O_2}'^{1/2} - P_{O_2}''^{1/2}) \quad (29)$$

with

$$\alpha = \frac{K_1}{16} [x - (8C_p^0 x + x^2)^{1/2} + 4C_p^0] \quad (30)$$

and

$$x = \frac{K_1}{2K_{-1}} (P_{O_2}'^{1/2} + P_{O_2}''^{1/2}) \quad (31)$$

For the very thin membranes with electrons contributing primarily to electronic conduction, oxygen permeation flux has the same form as of Eq. 29, but with a different α , as given below:

$$\alpha = \frac{K_{-1}}{P_{O_2}'^{1/2} + P_{O_2}''^{1/2}} \quad (32)$$

The results presented here show that α decreases with increasing oxygen pressure in the both cases.

Ionic-conducting membranes

For ionic conductors with small electronic conductivity contributed primarily by electron holes, $\sigma_i > \sigma_p$. With the Einstein's relation, it means:

$$C_V D_V \gg C_p D_p \quad (33)$$

In most ionic conductors, the concentration of the oxygen vacancy is much larger than that of electron, that is:

$$C_V \gg C_p \quad (34)$$

In this case, Eq. 15 is simplified to:

$$J_V = -\frac{1}{L} \int_{C_{V(l)}}^{C_{V(l)}} D_p dC_V \quad (35)$$

With Eqs. 20 and 21 and noting that $J_{O_2} = -J_V/2$, integrating Eq. 35 gives:

$$J_{O_2} = \frac{1}{4L} D_p (C_{p(l)} - C_{p(l)}) \quad (36)$$

Applying relation 34 to Eq. 16 also gives: $C_V \approx C_V^0$. Thus, using the following definitions:

$$C_{p(l)} = \left(\frac{K_1 C_V^0}{K_{-1}} \right)^{1/2} P_{O_2(l)}^{1/4} \quad (37)$$

$$C_{p(l)} = \left(\frac{K_1 C_V^0}{K_{-1}} \right)^{1/2} P_{O_2(l)}^{1/4} \quad (38)$$

and the surface parameter α :

$$\alpha = K_1 C_V^0 \quad (39)$$

Equations 18 and 19 can be written as:

$$J_{O_2} = \alpha (P_{O_2}'^{1/2} - P_{O_2(l)}^{1/2}) \quad (40)$$

and

$$J_{O_2} = \alpha (P_{O_2(l)}^{1/2} - P_{O_2}''^{1/2}) \quad (41)$$

With the equilibrium relation, such as Eq. 25, it can be readily shown that the electron-hole concentration at oxygen partial pressure of 1 atm is:

$$C_p^0 = \left(\frac{K_1 C_V^0}{K_{-1}} \right)^{1/2} \quad (42)$$

Inserting Eq. 37 and Eq. 38 into Eq. 36 and using the Einstein's relation, as well as Eq. 42, we obtain the following equation for the bulk electrochemical diffusion:

$$J_{O_2} = \frac{\beta}{L} (P_{O_2(l)}^{1/4} - P_{O_2(l)}^{1/4}) \quad (43)$$

Note $\beta = RT\sigma_p^0/4F^2$.

Equation 40, Eq. 41, and Eq. 43 can be solved simultaneously to give an equation correlating the oxygen permeation flux to P_{O_2}' , P_{O_2}'' , and the two rate constants, σ_p^0 and α . It is interesting to note that Eqs. 40, 41, 43 are similar to equations proposed by Dou et al. (1985) or Bouwmeester et al. (1992). However, the present analysis clearly shows the physical significance of the surface parameter α , which is proportional to the forward surface reaction rate constant for reaction E, as given by Eq. 39. Furthermore, the surface parameter α is shown to be the same for the both surface reactions. More importantly, α is independent of the oxygen partial pressure.

When the surface reaction is rate-limiting (smaller α and/or larger σ_p^0/L), $P_{O_2(l)} = P_{O_2(l)}$. Combination of Eq. 40 and Eq. 41 gives:

$$J_{O_2} = \frac{\alpha}{2} (P_{O_2}^{1/2} - P_{O_2}^{\prime\prime 1/2}) \quad (44)$$

which means that permeation flux is proportional to $P_{O_2}^{1/2}$. For the rate-limiting step of diffusion in the bulk oxide, $P_{O_2(l)} = P_{O_2}'$ and $P_{O_2(II)} = P_{O_2}^{\prime\prime}$. Equation 43 shows that the permeation flux is proportional to $P_{O_2}^{1/4}$.

For ionic conductors with electrons being responsible for the slight electronic conductivity, the following equation can be derived by the procedure similar to the one for Eq. 36:

$$J_{O_2} = \frac{D_n}{4L} (C_{n(II)} - C_{n(I)}) \quad (45)$$

We also define:

$$C_{n(I)} = \left(\frac{K_{-n}}{K_n C_V^0} \right)^{1/2} P_{O_2(l)}^{-1/4} \quad (46)$$

$$C_{n(II)} = \left(\frac{K_{-n}}{K_n C_V^0} \right)^{1/2} P_{O_2(II)}^{-1/4} \quad (47)$$

Inserting Eq. 46 and Eq. 47 into Eq. 45 and noting that $C_n^0 = (K_{-1}/(K_1 C_V^0))$, we obtain the following for oxygen permeation through the bulk oxide:

$$J_{O_2} = \frac{RT\alpha_n^0}{4F^2L} (P_{O_2(II)}^{-1/4} - P_{O_2(l)}^{-1/4}) \quad (48)$$

Applying Eq. 46 and Eq. 45 to Eq. 23 and Eq. 24, we obtain the following equations for the surface reactions:

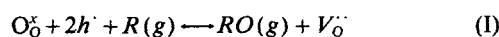
$$J_{O_2} = \frac{K_{-1}}{P_{O_2(l)}^{1/2}} (P_{O_2}^{\prime 1/2} - P_{O_2(l)}^{1/2}) \quad (49)$$

$$J_{O_2} = \frac{K_{-1}}{P_{O_2(II)}^{1/2}} (P_{O_2(II)}^{1/2} - P_{O_2}^{\prime\prime 1/2}) \quad (50)$$

Comparing the above two equations to Eq. 40 and Eq. 41, the surface permeation parameter α in this case decreases with increasing oxygen partial pressure.

Membranes with a reducing agent in low pressure side

In many cases, the permeate side of the dense oxide membrane is filled with a reducing agent, for example, hydrogen or methane. The oxygen permeates through the dense membrane and reacts with the reducing agent on interface II. For mixed conductors with electron hole primarily being responsible for the electronic conductivity, the surface reaction on interface II can be written as:



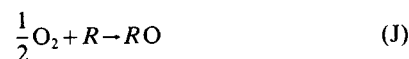
where R represents the reducing agent, which is involved in the surface charge transfer reaction.

Similarly, using the mass action law for reaction I gives:

$$J = K_R P_R C_{p(I)}^2 - K_{-R} P_{RO} C_{V(II)} \quad (51)$$

Thus, solving Eqs. 17, 18, 20, 21, and 51 simultaneously will give an implicit function connecting the permeation flux to P_{O_2}' , P_R , P_{RO} , and the rate constants associated with different rate steps.

For the ionic conductors, $C_{V(II)} \approx C_V^0$. Defining an oxygen partial pressure $P_{O_2}^{\prime\prime}$ in the permeate side as a value equilibrated with P_R and P_{RO} of the following chemical reaction:



we obtain:

$$P_{RO} = K_e P_R P_{O_2}^{\prime\prime 1/2} \quad (52)$$

where K_e is the equilibrium constant of reaction J. We also define:

$$C_{p(II)} = \sqrt{\frac{K_{-R} C_V^0 K_e}{K_R}} P_{O_2(II)}^{1/4} = \sqrt{\frac{K_1 C_V^0}{K_{-1}}} P_{O_2(II)}^{1/4} \quad (53)$$

Inserting Eqs. 52 and 53 into Eq. 51 yields:

$$J = \alpha_R (P_{O_2(l)}^{1/2} - P_{O_2}^{\prime\prime 1/2}) \quad (54a)$$

$$\alpha_R = K_e C_V^0 K_{-R} P_R \quad (54b)$$

Equation 40, Eq. 43, and Eq. 54 govern the oxygen permeation through the ionic-conducting membranes with a reducing agent in the permeate side. It is important to note that in this case the surface permeation parameter on interface II is different from that on interface I.

Relationship between O^{18} - O^{16} exchange rate constant k_s and oxygen surface permeation parameter α

The O^{16} - O^{18} isotope exchange between the solid phase and gas phase has been employed to study the surface reaction rate under equilibrium conditions (Steele et al., 1987; Boukamp et al., 1989). In this method, an ionic-conducting solid oxide (normally powder) with known surface area is first equilibrated with an atmosphere containing one isotope of oxygen (for example, O_2^{16}). At time zero, the atmosphere is changed to another isotope of oxygen (for example, O_2^{18}) with the same oxygen pressure, and the concentration of O_2^{16} or O_2^{18} in the atmosphere is monitored as a function of time. The oxygen exchange flux of O^{18} (in moles of O_2^{18}) is correlated to the exchange rate constant k_s by (Steele et al., 1987; Boukamp et al., 1989; Vinke, 1991):

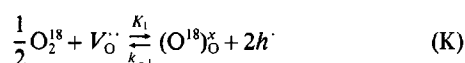
$$J_{ex} = k_s (R_g^{18} - R_s^{18}) \quad (55)$$

where R_g^{18} and R_s^{18} are fraction of O^{18} in the gas phase and the solid oxide, respectively.

Considering the surface charge transfer reaction as shown by reaction E as being under the equilibrium conditions in the isotope exchange experiment, we have the following equilibrium relation for the ionic conductors:

$$K_1 P_{O_2}^{1/2} C_V^0 = k_{-1} [O_O^x] C_p^2 \quad (56)$$

where $[O_O^x]$ is the lattice oxygen concentration, and P_{O_2} is the oxygen pressure in the atmosphere. For O^{18} exchange between the gas phase and the solid oxide, it follows:



The O^{18} exchange flux is expressed by the mass action law as:

$$J_{ex} = K_1 P_{O_2}^{1/2} R_g^{18} C_V^0 - k_{-1} [O^{18}]_O^x C_p^2 \quad (57)$$

where $[O^{18}]_O^x$ is the concentration of O^{18} in the lattice. Combining Eq. 56 and Eq. 57 and noting that $R_s^{18} = [O^{18}]_O^x / [O_O^x]$ give:

$$J_{ex} = k_s C_V^0 P_{O_2}^{1/2} [R_s^{18} - R_s^{18}] \quad (58)$$

Combining Eq. 58 with Eq. 55 and Eq. 40 indicates:

$$k_s = \alpha P_{O_2}^{1/2} \quad (59)$$

Equation 59 is significant in the sense that it theoretically correlates the two experimentally measurable rate constants, one measured under equilibrium conditions, and the other under dynamic conditions. Since measurements of α by permeation method normally require very thin membranes, which are difficult to fabricate, Eq. 59 suggests a method that is based on the measurements of isotope exchange rate constant k_s of the powdered material, for measuring oxygen surface permeation parameter α .

Comparison with Experimental Data

Experimental data ideal for the comparison are the oxygen permeation fluxes through thin (preferably smaller than 50 μm) dense oxide membranes of different thickness measured at different oxygen partial pressures and temperatures. However, it is well known that obtaining these data is very difficult because: (1) to fabricate gas-tight (but oxygen permeable) thin (< 50 μm) mixed-conducting oxide membranes (supported on porous supports) for the oxygen permeation measurements is still a technical challenge; (2) high temperature (> 700°C) sealing needed for the high temperature oxygen permeation measurements (sealing dense-porous membrane composites) is still an unsolved problem. As a result, experimental data on oxygen permeation through thin dense oxide membranes, especially with different membrane thickness, are very scarce. Results of the theoretical development presented in this article are compared next with limited available experimental data to illustrate the application of this new approach. It is not attempted to explain all the experimental data reported in the literature, as this is beyond the scope of this article.

Dou et al. (1985) measured oxygen permeation through calcia-stabilized zirconia membrane (CSZ, an oxygen ionic-conductor) of various thickness (500–2,000 μm). They used the empirical equations, Eqs. 4 and 5, which have the following solution ($P_{O_2}'' \approx 0$):

$$J_{O_2} = \frac{\beta^2}{2L^2\alpha} \left[\left(1 + \frac{4L^2\alpha^2}{\beta^2} P_{O_2}'^{1/2} \right)^{1/2} - 1 \right] \quad (60)$$

Table 1. Constants of Oxygen Permeation through Calcia Stabilized Zirconia Membrane at 1,230°C

P_{O_2}' (atm)	$\alpha \times 10^9$ (mol/cm ² ·s·atm ^{1/2})		$\beta \times 10^{10}$ (mol/cm·s·atm ^{1/4})	
	Model of Dou et al.	Present Model	Model of Dou et al.	Present Model
1.0	0.94	2.35	1.33	2.13
0.21	1.01	2.38	1.21	2.14

* α in Eq. 4 is 1/2 of α defined by Dou et al.

to describe the experimental data. At a given P_{O_2}' , α and β were obtained by regressing the experimental J_{O_2} with Eq. 60 at three different membrane thickness. The experimental data were well fitted by Eq. 60. However, the fitted α increased and β decreased with decreasing P_{O_2}' (see Table 1). This reflects the empirical nature of the equations used to describe the experiments. The results of this new theoretical development show that Eqs. 40, 41, and 43 are the equations consisting of constants with physical significance for the permeation systems studied by Dou et al. To ensure the accuracy of experimental data, the oxygen permeation data at highest temperature (1,230°C) and P_{O_2}' (0.21 atm, 1 atm) reported by Dou et al. are compared with the new theoretical model, Eqs. 40, 41, and 43. The Powell hybrid method (Kahaner et al., 1989) was used to solve the nonlinear algebraic equations (Eqs. 40, 41, and 43) to give $J_{O_2} = f(\alpha, \beta, P_{O_2}', L)$ ($P_{O_2}'' \approx 0$). Values of the new constants α and β were found by fitting J_{O_2} (theoretical) with J_{O_2} (experimental) at three different thicknesses (500, 1,650, 1,940 μm). The method of quasi-Newton with line search (Kahaner et al., 1989) was employed in the nonlinear least-squared regression.

The fitting results are presented in Figure 2 and Table 1. As shown in Figure 2, the new model describes well the experimental data. The parameters α and β found with this new model are independent of P_{O_2}' , as given in Table 1. This is consistent with the physical meaning of these two parameters defined in the mechanism proposed for the development of Eqs. 40, 41, and 43.

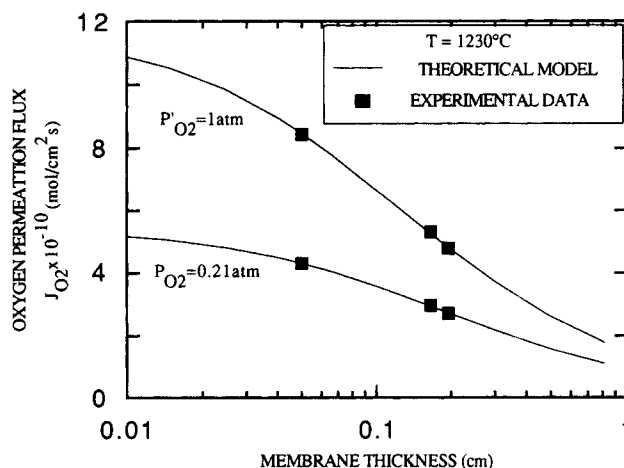
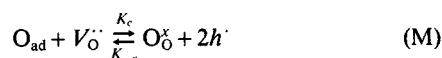
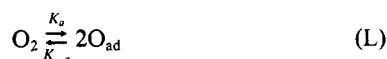


Figure 2. Oxygen permeation through calcia stabilized zirconia membrane: experimental data of Dou et al. (1985) vs. theoretical model with physical significance (Eqs. 40, 41, 43).

Bouwmeester et al. (1992) reported excellent experimental data on oxygen permeation through 25 mol % erbia-stabilized bismuth oxide (BE25) membranes of three different thickness (200, 700, 2,850 μm). They employed the empirical equations, Eqs. 6–8, to analyze the experimental data. Although the experimental data can be well described by Eqs. 6–8, the order 5/8 on P_{O_2} and constant α in Eqs. 6 and 8 do not have physical meaning. Thus, the value 5/8 and constant α should be considered as the apparent order and permeation constant for the surface reactions. With the new approach reported in this article, it is possible to derive the oxygen permeation equations for the permeation systems studied by Bouwmeester et al. (1992).

As mentioned earlier, the surface reaction E may involve several substeps. Thus, a possible mechanism for the surface reaction in the oxygen permeation through the BE 25 membrane consists of the following adsorption and charge transfer reaction (on interface I):



where O_{ad} indicates the adsorbed atomic oxygen on interface I. Applying the mass action law to reactions L and M gives:

$$J_{\text{O}_2} = K_a P_{\text{O}_2} - K_{-a} [\text{O}_{\text{ad}}]^2 \quad (61)$$

$$J_{\text{O}_2} = K_c C_V^0 [\text{O}_{\text{ad}}] - K_{-c} C_{p(l)}^2 \quad (62)$$

Inserting the following definition into Eqs. 61 and 62:

$$C_{p(l)} = \left[\frac{K_c}{K_{-c}} \left(\frac{K_a}{K_{-a}} \right)^{1/2} C_V^0 \right]^{1/2} P_{\text{O}_2(l)}^{1/4} \quad (63)$$

$$[\text{O}_{\text{ad}}] = \left(\frac{K_a}{K_{-a}} \right)^{1/2} P_{\text{O}_2(\text{ad})}^{1/2} \quad (64)$$

one obtains:

$$J_{\text{O}_2} = \gamma (P_{\text{O}_2} - P_{\text{O}_2(\text{ad})}) \quad (65)$$

$$J_{\text{O}_2} = \alpha (P_{\text{O}_2(l)}^{1/2} - P_{\text{O}_2(\text{de})}^{1/2}) \quad (66)$$

where $\gamma = K_a$, the adsorption rate constant and:

$$\alpha = K_c \left(\frac{K_a}{K_{-a}} \right)^{1/2} C_V^0 = K_1 C_V^0$$

Similar reactions can be proposed for surface reactions on interface II. The final results are:

$$J_{\text{O}_2} = \alpha (P_{\text{O}_2(\text{II})}^{1/2} - P_{\text{O}_2(\text{de})}^{1/2}) \quad (67)$$

$$J_{\text{O}_2} = \gamma (P_{\text{O}_2(\text{de})} - P_{\text{O}_2}) \quad (68)$$

Equations 65, 66, 43, 67, and 68 are the new model for oxygen

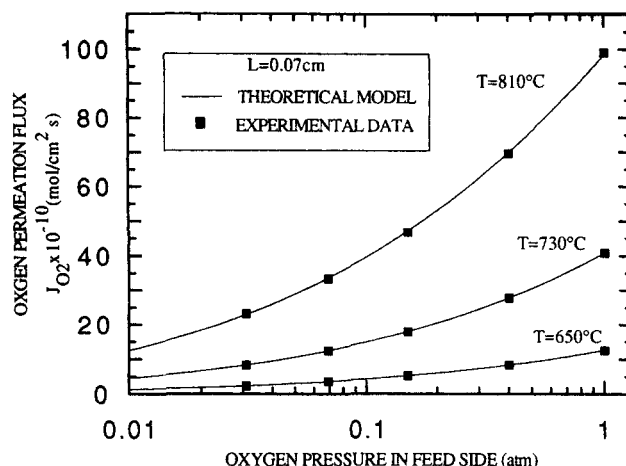


Figure 3. Oxygen permeation through erbia stabilized bismuth oxide membrane: experimental data of Bouwmeester et al. (1992) vs. theoretical model with physical significance (Eqs. 64–67 and Eq. 43).

permeation through ionic-conducting BE 25 membranes. Note that for very large γ or small α , this model becomes identical to the simplified model of Eqs. 40, 41, and 43.

The new model was compared with the experimental data of Bouwmeester et al. (1992). Values of constants α , β , and γ in the new model were calculated by regressing the solution of Eqs. 65, 66, 43, 67 and 68 with experimental permeation fluxes at five different P_{O_2} (0.031, 0.069, 0.15, 0.40, 1 atm) for the BE 25 membrane of 700 μm thick. Again, same methods reported by Kahaner et al. (1989) were used to solve the five nonlinear algebraic equations [to give $J_{\text{O}_2} = f(\alpha, \beta, \gamma, L, P_{\text{O}_2}, P_{\text{O}_2})$] and to perform the nonlinear least-squared regression (to obtain α, β, γ). In Figure 3, the calculated results are compared with the experimental permeation data at three different temperatures. As shown in the figure, the new model agrees well with the experimental results. The corresponding values of α, β , and γ at three different temperatures are listed in Table 2. Values of α and β obtained by Bouwmeester et al. (1992) using the empirical model are also given in Table 2 for comparison.

Although both the empirical model and the new model agree well with the experimental data, the new model clearly illustrates the physical meaning of the rate steps and the associated parameters. The rate constants α, β, γ can be well described by the Arrhenius equation, as shown in Figure 4. The resulting preexponential factor and activation energy for each rate con-

Table 2. Constants of Oxygen Permeation through Erbia Stabilized Bismuth Oxide Membrane

T (°C)	$\alpha \times 10^8$ (mol/cm ² ·s·atm ^{1/2})		$\beta \times 10^9$ (mol/cm ² ·s·atm ^{1/4})		$\gamma \times 10^7$ (mol/cm ² ·s·atm)
	Model of Bouwmeester	Present Model	Model of Bouwmeester	Present Model	Present Model
650	0.556	0.390	0.444	0.454	2.89
730	2.16	1.95	1.19	0.845	5.04
810	7.26	13.7	2.88	1.29	8.12

* The unit of α in the Bouwmeester model is mol/cm²·s·atm^{5/8}.

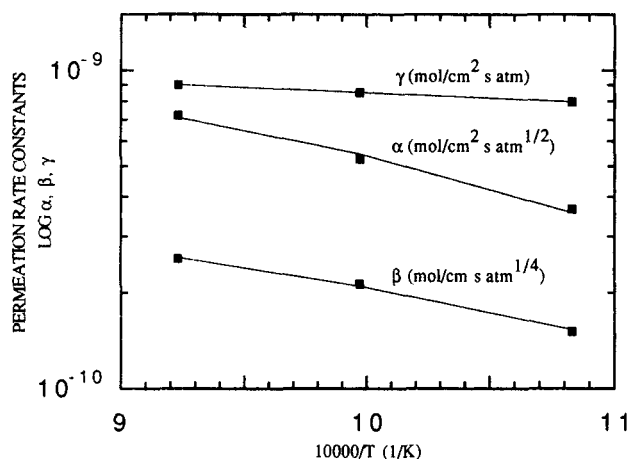


Figure 4. Arrhenius plots of permeation rate constants α , β and γ in the theoretical model for erbia stabilized bismuth oxide membrane.

stants are given in Table 3. It is expected that the activation energy for the charge transfer reaction (reaction M) is larger than that for bulk diffusion and adsorption of oxygen, which is indeed so as shown by the data given in Table 3. The comparison between the new model and experimental data indicate that both adsorption (or desorption) of oxygen and charge transfer steps are important in the surface reactions for oxygen permeation through the BE25 membranes.

The only published oxygen permeation data for thin ($< 50 \mu\text{m}$) dense oxide membranes appear to be those recently reported by Lin et al. (1992) on electrochemical vapor deposited yttria stabilized zirconia (YSZ) membrane. The experimentally measured J_{O_2} ranges from $0.9\text{--}1.2 \times 10^{-8} \text{ mol/cm}^2 \cdot \text{s}$ for $5 \mu\text{m}$ thick YSZ membrane at $1,000^\circ\text{C}$ ($P_{\text{O}_2} = 0.03 \text{ atm}$, $P_{\text{O}_2}' \approx 10^{-5} \text{ atm}$). Because of the unavailability of α value for YSZ membrane, it was previously attempted to use α value of Dou et al. (1985) for CSZ membrane to describe the permeation flux (Lin et al., 1990). A simple calculation using $\alpha = 2.35$ for CSZ membrane (see Table 1) shows that in this case the surface reaction would be the rate limiting step for $5 \mu\text{m}$ thick YSZ membrane, with a predicted J_{O_2} of about $2.0 \times 10^{-10} \text{ mol/cm}^2 \cdot \text{s}$. This could not explain the experimental data.

However, the theoretical result (Eq. 59) suggests that the surface permeation parameter α can be calculated from the $\text{O}^{16}\text{--O}^{18}$ exchange coefficient k_s . Gellings and Bouwmeester (1992) reported k_s of about $9 \times 10^{-10} \text{ mol/cm}^2 \cdot \text{s}$ for YSZ at 700°C and $P_{\text{O}_2} = 0.21 \text{ atm}$, which gives about $2 \times 10^{-9} \text{ mol/cm}^2 \cdot \text{s} \cdot \text{atm}^{1/2}$ for α using Eq. 59. A value of $5 \times 10^{-7} \text{ mol/cm}^2 \cdot \text{s} \cdot \text{atm}^{1/2}$ for α at $1,000^\circ\text{C}$ for YSZ can be calculated using the activation energy of 191 kJ/mol (the same as for CSZ

Table 3. Preexponential Factor and Activation Energy for Rate Constants α , β , and γ for Oxygen Permeation through Erbia Stabilized Bismuth Oxide Membrane

	Preexponential Factor	Activation Energy
α for Charge Transfer	$91.72 \text{ mol/cm}^2 \cdot \text{s} \cdot \text{atm}^{1/2}$	184 kJ/mol
β for Bulk Diffusion	$5.66 \times 10^{-7} \text{ mol/cm} \cdot \text{s} \cdot \text{atm}^{1/4}$	54.6 kJ/mol
γ for Adsorption	$3.14 \times 10^{-4} \text{ mol/cm}^2 \cdot \text{s} \cdot \text{atm}$	53.7 kJ/mol

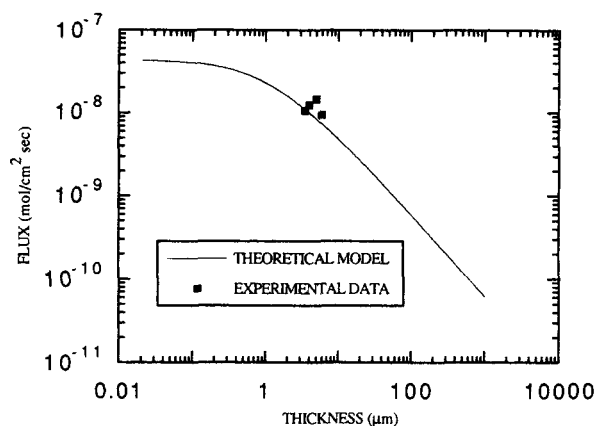


Figure 5. Dependence of oxygen permeation flux on the membrane thickness for yttria stabilized zirconia membranes, predicted from experimental α and β values.

Experimental oxygen permeation data for ultrathin YSZ membrane prepared by Lin et al. (1992) are consistent with the theoretical model.

reported by Dou et al., 1985; similar to that for BE 25, see Table 3). Furthermore, β value of $1.6 \times 10^{-11} \text{ mol/cm} \cdot \text{s} \cdot \text{atm}^{1/4}$ for YSZ at $1,000^\circ\text{C}$ can be found from electron-hole conductivity data ($\sigma_p^0 = 5.8 \times 10^{-5} \text{ ohm}^{-1} \cdot \text{cm}^{-1} \cdot \text{atm}^{-1/4}$) (Park and Blumenthal, 1989). With these values of α and β , theoretical value of J_{O_2} were calculated using Eqs. 40, 41, and 43, and are plotted against different thickness in Figure 5. The experimental data of Lin et al. (1992) are also given in Figure 5, which shows a good consistency between the experimental data and predicted data using the α value calculated from k_s . Also Gellings and Bouwmeester (1992) reported k_s values for BE25 at 600°C and 800°C . α values, calculated from k_s using Eq. 59, range from 2.69×10^{-9} (at 600°C) to 1.22×10^{-7} (800°C) $\text{mol/cm}^2 \cdot \text{s} \cdot \text{atm}^{1/2}$, which are consistent with the (apparent) α values measured by oxygen permeation method (see Table 2).

Conclusions

- A new theoretical approach different from the conventional Wagner method was presented for the development of fundamental equations governing oxygen permeation through thin ionic-electronic mixed conducting solid oxide membranes. Both the bulk diffusion and the surface reactions were considered in this theoretical development. In general cases, the final result is an implicit equation correlating the oxygen permeation flux to the driving force, membrane thickness, and rate constants in each step with physical significance.

- For a mixed-conducting membrane with both bulk diffusion resistance and surface reaction resistance, the dependence of the oxygen permeation flux on oxygen partial pressure, membrane thickness, and temperature is fairly complex, depending on the detailed mechanism in the surface reactions and values of the rate parameters involved. This dependence can be predicted using the fundamental equations presented.

- Application of these fundamental equations to some special cases (mixed-conducting membranes with a rate-limiting step, ionic-conducting membranes, ionic-conducting membranes with a reducing agent) leads to simpler equations cor-

relating oxygen permeation flux to the driving force, membrane thickness, and rate constants with physical significance.

- It was shown that for ionic conductors the surface permeation parameter measured by dynamic oxygen permeation method, α , is directly related to the $O^{18}-O^{16}$ exchange rate constant measured under equilibrium conditions, k_s , which is $k_s = \alpha P_{O_2}^{1/2}$.

- The oxygen permeation equations derived using this theoretical approach were compared with experimental permeation data and the theoretical results agree well with the experimental data. With this approach, it is possible to find a detailed surface reaction mechanism by comparing the permeation flux equation, derived from an assumed mechanism, with the experimental permeation data.

Acknowledgment

The authors are grateful to the financial support on this project from the National Science Foundation (CTS-9208518) and Amoco Natural Gas Research Program.

Notation

- a_i = activity of i species
- C_i = concentration of i species
- C_i^0 = concentration of i species in solid oxide equilibrated to an atmosphere having 1 atm oxygen partial pressure
- D_a = apparent diffusion coefficient, Eq. 9
- D_i = diffusion coefficient of i species
- e' = electron
- f_i = thermodynamic factor of i species, Eq. A10
- F = Faraday's constant
- h^0 = electron hole
- J_{ex} = exchange flux of O_2^{18}
- J_i = flux of i species
- k_{-1} = backward reaction rate constant
- k_s = $O_2^{16}-O_2^{18}$ exchange rate constant
- K_1 = forward reaction rate constant for surface reaction E, Eq. 18
- K_{-1} = backward reaction rate constant for surface reaction including lattice oxygen concentration for surface reaction E, Eq. 18
- K_a = forward reaction constant for adsorption, Eq. 61
- K_{-a} = backward reaction constant for adsorption, Eq. 61
- K_c = forward reaction constant for charge transfer reaction, Eq. 62
- K_{-c} = backward reaction rate constant for charge transfer reaction including lattice oxygen concentration, Eq. 62
- K_e = equilibrium constant of reaction J
- K_n = forward reaction rate constant for surface reaction G, Eq. 23
- K_{-n} = backward reaction rate constant for surface reaction G, Eq. 23
- K_R = forward reaction rate constant for surface reaction with reducing agent, Eq. 51
- K_{-R} = backward reaction rate constant for surface reaction with reducing agent, Eq. 51
- L = film thickness
- O_O^x = lattice oxygen
- $[O_O^x]$ = lattice oxygen concentration
- P_{O_2} = oxygen partial pressure at retentate side (higher pressure side)
- P_{O_2}'' = oxygen partial pressure at permeate side (lower pressure side)
- $P_{O_2}^*$ = partial pressure of the hypothetical neutral molecular oxygen
- $P_{O_2(ad)}$ = quantity related to the concentration of adsorbed oxygen on interface I, Eq. 65
- $P_{O_2(de)}$ = quantity related to the concentration of adsorbed oxygen on interface II, Eq. 67
- $P_{O_2(l)}$ = quantity related to $C_{p(l)}$ or $C_{n(l)}$, defined by Eqs. 37 and 46

- $P_{O_2(l)}$ = quantity related to $C_{p(l)}$ or $C_{n(l)}$, defined by Eqs. 38 and 57 or Eq. 53
- R = gas constant
- t_i = transfer number of ion
- t_n = transfer number of electron
- T = temperature
- $V_O^{\bullet\bullet}$ = oxygen vacancy
- z_i = charge number of i species

Greek letters

- α = surface permeation constant
- β = bulk permeation coefficient, Eq. 3
- μ_i = chemical potential of i species
- $\nabla\mu_i$ = chemical potential gradient
- σ_i = conductivity of i species
- σ_i^0 = conductivity of i species in metal oxide exposed at an atmosphere having 1 atm oxygen partial pressure
- σ_t = total conductivity
- $\nabla\phi$ = electric field gradient

Subscripts

- ad = for oxygen adsorbed on interface I
- de = for oxygen adsorbed on interface II
- g = for gas phase
- n = for electron
- O_2 = for neutral molecular oxygen
- p = for electron hole
- R = for reducing agent
- s = for solid phase
- V = for oxygen vacancy
- (I) = for interface I (higher pressure side)
- (II) = for interface II (lower pressure side)

Superscripts

- x = for neutral species
- ' = for negative charged species
- \cdot = for positive charged species
- 0 = for membrane equilibrated with the atmosphere of 1 atm oxygen partial pressure

Literature Cited

- Alcock, C. B., and J. C. Chan, "The Oxygen Permeability of Stabilized Zirconia Electrolytes at High Temperatures," *Canad. Met. Quarterly*, **11**, 559 (1972).
- Bhave, R. R., *Inorganic Membranes, Synthesis, Characterization and Applications*, Van Nostrand Reinhold, New York (1991).
- Boukamp, B. A., I. C. Vinke, K. J. de Vries, and A. J. Burggraaf, "Surface Oxygen Exchange Properties of Bismuth Oxide-Based Solid Electrolytes and Electrode Materials," *Solid State Ionics*, **32/33**, 918 (1989a).
- Boukamp, B. A., K. J. de Vries, and A. J. Burggraaf, "Surface Oxygen Exchange in Bismuth Oxide Based Materials," in *Non-Stoichiometric Compounds, Surface, Grain Boundaries and Structural Defects*, J. Nowotny and W. Weppner, Kluwer, Boston, eds., p. 299 (1989b).
- Bouwmeester, H. J. M., H. Kruidhof, A. J. Burggraaf, and P. J. Gellings, "Oxygen Semipermeability of Ebia-Stabilized Bismuth Oxide," *Solid State Ionics*, **53**, 460 (1992).
- Brian, R., "Fabrication of Solid Oxide Fuel Cell by Electrochemical Vapor Deposition," U.S. Patent 4,831,965 (1989).
- Burggraaf, A. J., K. Keizer, and B. A. van Hassel, "Ceramic Nanostructure Materials, Membranes and Composites," *Solid State Ionics*, **32/33**, 771 (1989).
- Burggraaf, A. J., H. J. M. Bouwmeester, B. A. Boukamp, R. J. R. Uhlhorn, and V. T. Zaspalis, "Synthesis, Microstructure and Properties of Porous and Dense Ceramic Membranes," in *Science of Ceramic Interface*, J. Nowotny, ed., Elsevier, Amsterdam, p. 525 (1991).
- Burggraaf, A. J., and Y. S. Lin, "Method for Manufacturing Ultrathin Inorganic Membranes," U.S. Patent 5, 160, 618 (1992).

- Carolan, M. F., and J. N. Michaels, "Growth Rate and Mechanism of Electrochemical Vapor Deposited Yttria-Stabilized Zirconia Film," *Solid State Ionics*, **37**, 189 (1990).
- Dou, S., C. R. Masson, and P. D. Pacey, "Mechanism of Oxygen Permeation through Lime-Stabilized Zirconia," *J. Electrochem. Soc.*, **132**, 1843 (1985).
- Fouletier, J., P. Fabry, and M. Kleitz, "Electrochemical Semipermeability and Electrode Microsystem in Solid Oxide Electrolyte Cells," *J. Electrochem. Soc.*, **123**, 204 (1976).
- Gellings, P. J., and H. J. M. Bouwmeester, "Ion and Mixed Conducting Oxides as Catalysis," *Catal. Today*, **12** (1992).
- Gür, T. M., A. Belzner, and R. A. Huggins, "A New Class of Oxygen Selective Chemically Driven Nonporous Ceramic Membranes: I. A-site Doped Perovskites," *J. Membr. Sci.*, **75**, 151 (1992).
- Hazbun, E. A., "Ceramic Membrane for Hydrocarbon Conversion," U.S. Patent 4,791,079 (1988).
- Hazbun, E. A., "Ceramic Membrane and Use Thereof for Hydrocarbon Conversion," U.S. Patent 4,827,071 (1989).
- Heyne, L., "Ionic Conductivity in Oxides," in *Mass Transfer in Oxides*, L. Heyne et al., eds., National Bureau of Standards, Washington, DC, No. 296, p. 149 (1968).
- Heyne, L., "Electrochemistry of Mixed Ionic-Electronic Conductors," in *Solid Electrolytes*, S. Geller, ed., Springer-Verlag, New York, p. 167 (1977).
- Hsieh, H. P., "Inorganic Membrane Reactors," *Catal. Rev.-Sci. Eng.*, **33**, 1 (1991).
- Isenburg, A. O., "Energy Conversion via Solid Oxide Electrolyte Electrochemical Cells at High Temperatures," *Solid State Ionics*, **3/4**, 431 (1981).
- Kahaner, D., C. Moler, and S. Nash, *Numerical Method and Software*, Prentice-Hall, Englewood Cliffs, NJ (1989).
- Kingery, W. D., H. K. Bowen, and D. R. Uhlmann, *Introduction to Ceramics*, Chap. 4, Wiley, New York (1976).
- Kofstad, P., *High-Temperature Oxidation of Metals*, Chap. V, Wiley, New York (1966).
- Kofstad, P., *Nonstoichiometry, Diffusion and Electrical Conductivity in Binary Metal Oxides*, Wiley, New York (1972).
- Kröger, F. A., and V. J. Vink, "Relations Between the Concentrations of Imperfections in Crystalline Solid," *Solid State Physics*, **3**, F. Seitz and D. Turnbull, eds., Academic Press, New York, p. 307 (1956).
- Lin, Y. S., L. G. J. de Haart, K. J. de Vries, and A. J. Burggraaf, "A Kinetic Study of the Electrochemical Vapor Deposition of Solid Oxide Electrolyte Films on Porous Substrates," *J. Electrochem. Soc.*, **137**, 3960 (1990).
- Lin, Y. S., K. J. de Vries, H. W. Brinkman, and A. J. Burggraaf, "Oxygen Semipermeable Solid Oxide Membrane Composites Prepared by Electrochemical Vapor Deposition," *J. Membr. Sci.*, **66**, 211 (1992).
- Lin, Y. S., "Porous and Dense Inorganic Membranes for Gas Separation," Preprint Volume, 1992 Annual AIChE Meeting 1st Separation Topical Conference, J. L. Humphrey, ed., AIChE, New York, p. 843 (1992).
- Pal, U. B., and S. C. Singhal, "Electrochemical Vapor Deposition of Yttria-Stabilized Zirconia Films," *J. Electrochem. Soc.*, **137**, 2937 (1990).
- Palgouev, S. F., V. K. Gilderman, and A. D. Neujmin, "Oxygen Permeability of Stabilized Zirconia," *J. Electrochem. Soc.*, **122**, 745 (1972).
- Park, J. H., and R. N. Blumenthal, "Electronic Transport in 8 Mole Percent $\text{Y}_2\text{O}_3\text{-ZrO}_2$," *J. Electrochem. Soc.*, **136**, 2867 (1989).
- Robertson, N. L., and J. N. Michaels, "Surface Diffusion Limited Oxygen Exchange in Zirconia Electrochemical Cells," *AIChE Symp. Ser.*, **83**(254), 56 (1987).
- Steele, B. C. H., T. A. Kilner, P. F. Dennis, A. E. McHale, M. van Hemert, and A. J. Burggraaf, "Oxygen Surface Exchange and Diffusion in Fast Ionic Conductors," *Solid State Ionics*, **18/19**, 1038 (1986).
- Steele, B. C. H., *Ceramic Electrochemical Reactors, Current Status and Application*, Ceramionics, London (1987).
- Van Hassel, B. A., "Transport and Oxygen Transfer Properties of Ion Implanted Yttria Stabilized Zirconia," PhD Thesis, Univ. of Twente, The Netherlands (1990).
- Vinke, I. C., "Electrochemical and Electrode Properties of Stabilized Bismuth Oxide Ceramics," PhD Thesis, Univ. of Twente, The Netherlands (1991).

Appendix: Equations for Bulk Diffusion in Dense Oxide Membranes

The particle fluxes of the two charged species can be described by (Heyne, 1977; Kofstad, 1972):

$$J_1 = -\frac{\sigma_1}{z_1^2 F^2} (\nabla \mu_1 + z_1 F \nabla \phi) \quad (\text{A1})$$

$$J_2 = -\frac{\sigma_2}{z_2^2 F^2} (\nabla \mu_2 + z_2 F \nabla \phi) \quad (\text{A2})$$

where $\nabla \phi$ is the electric field gradient, and $\nabla \mu_i$ and z_i are chemical potential gradient and charge number for the charged species i ($i = 1, 2$). For membrane, there is no external current, so the following correlation applies at steady state:

$$z_1 J_1 + z_2 J_2 = 0 \quad (\text{A3})$$

combination of Eqs. A1-A3 yields:

$$J_1 = -\frac{\sigma_1 \sigma_2}{(\sigma_1 + \sigma_2) z_1^2 F^2} \left(\nabla \mu_1 - \frac{z_1}{z_2} \nabla \mu_2 \right) \quad (\text{A4})$$

In the Wagner theory, a quasi-equilibrium is assumed between the electron (charged species 2), oxygen ion (charged species 1), and neutral oxygen (that is, $1/2 \text{O}_2 = \text{O}^\bullet - 2e$), so:

$$\frac{1}{2} \nabla \mu_{\text{O}_2} = \nabla \mu_1 - 2 \nabla \mu_2 \quad (\text{A5})$$

Substituting Eq. A5 into Eq. A4 gives:

$$J_1 = -\frac{\sigma_1 \sigma_2}{8(\sigma_1 + \sigma_2) F^2} \nabla \mu_{\text{O}_2} \quad (\text{A6})$$

Noting that $J_{\text{O}_2} = J_1/2$ in this case and $t_1 = \sigma_1/\sigma_t$ and $t_n = \sigma_2/\sigma_t$, Eq. A6 is identical to Eq. 1 for oxygen permeation in one-dimensional membrane system.

For general cases, the conductivity and chemical potential can be correlated to the concentrations and diffusivities of the charged species by:

$$\sigma_i = \frac{z_i^2 F^2}{RT} C_i D_i \quad (\text{Einstein's relation}) \quad (\text{A7})$$

and

$$\nabla \mu_i = \frac{RT}{C_i} \left(\frac{\partial \ln a_i}{\partial \ln C_i} \right) \nabla C_i \quad (\text{A8})$$

with these equations we can rearrange Eq. A4 to:

$$J_1 = -\frac{z_2^2 C_1 D_1 C_2 D_2}{z_1^2 C_1 D_1 + z_2^2 C_2 D_2} \left(f_1 \frac{\nabla C_1}{C_1} - f_2 \frac{z_1}{z_2} \frac{\nabla C_2}{C_2} \right) \quad (\text{A9})$$

where

$$f_i = \frac{\partial \ln a_i}{\partial \ln C_i} \quad (i = 1 \text{ or } 2) \quad (\text{A10})$$

and is called the thermodynamic factor (Heyne, 1977). In general, f_i is a function of C_1 and C_2 . It becomes unity for ideal behavior.

For oxygen permeation through the oxide membrane at steady state, local electric neutrality is required in the bulk oxides. Mathematically, it means that the change of the concentration of the two mobile charged species should be correlated by:

$$\frac{dC_1}{dC_2} = -\frac{z_2}{z_1} \quad (\text{A11})$$

Equation A11 also gives:

$$z_1 C_1 + z_2 C_2 = z_1 C_1^0 + z_2 C_2^0 \quad (\text{A12})$$

where C_1^0 and C_2^0 are the equilibrium concentrations of the two mobile charged species when the oxide membrane is equilibrated to an ambient atmosphere of 1 atm oxygen partial pressure. Values of C_1^0 and C_2^0 depend on the mechanism of defect formation of the oxide membrane. For defect formation reaction A, the equilibrium oxygen vacancy concentration is about half of the doped yttrium concentration:

$$C_V^0 \approx \frac{1}{2} [Y'_{Zr}] \quad (\text{A13})$$

Equation A11 can be also written as:

$$\nabla C_2 = -\frac{z_1}{z_2} \nabla C_1 \quad (\text{A14})$$

Substitution of Eq. A14 into Eq. A9 gives Eqs. 9 and 10.

Manuscript received Dec. 28, 1992, and revision received Aug. 5, 1993.